Earthq Eng & Eng Vib (2014) 13: 695-705 **DOI**:10.1007/s11803-014-0273-6

Vector-intensity measure based seismic vulnerability analysis of bridge structures

Li Zhongxian[1, 2†], Li Yang[1‡] and Li Ning[1, 2§]

1. *School of Civil Engineering, Tianjin University, Tianjin 300072, China*

2. *Key Laboratory of Coast Civil Structure Safety, Ministry of Education, Tianjin 300072, China*

Abstract: This paper presents a method for seismic vulnerability analysis of bridge structures based on vector-valued intensity measure (vIM), which predicts the limit-state capacities efficiently with multi-intensity measures of seismic event. Accounting for the uncertainties of the bridge model, ten single-bent overpass bridge structures are taken as samples statistically using Latin hypercube sampling approach. 200 earthquake records are chosen randomly for the uncertainties of ground motions according to the site condition of the bridges. The uncertainties of structural capacity and seismic demand are evaluated with the ratios of demand to capacity in different damage state. By comparing the relative importance of different intensity measures, $S_a(T_1)$ and $S_a(T_2)$ are chosen as vIM. Then, the vector-valued fragility functions of different bridge components are developed. Finally, the system-level vulnerability of the bridge based on vIM is studied with Dunnett-Sobel class correlation matrix which can consider the correlation effects of different bridge components. The study indicates that an increment IMs from a scalar IM to vIM results in a significant reduction in the dispersion of fragility functions and in the uncertainties in evaluating earthquake risk. The feasibility and validity of the proposed vulnerability analysis method is validated and the bridge is more vulnerable than any components.

Keywords: bridge structure; seismic vulnerability analysis; vector-valued intensity measure; components′ correlation; system vulnerability

1 Introduction

As an important part of social infrastructures, bridge plays a crucial role in transportation and earthquake relief. The damage of bridges caused by earthquake often lead to traffic interruption, which will not only affect people′s normal life and economic operation, resulting in serious economic losses, but also bring great difficulties to earthquake relief work. Thus, studies on the seismic performance of bridge subjecting earthquake excitation are particularly important. Due to the uncertainties of ground motions and bridge dynamic characteristics, probabilistic methods were adopted in the evaluation of seismic performance of bridge structures widely. In this context, a basic framework of probabilistic methods for seismic design and evaluation based on performance is proposed at the Pacific Earthquake Engineering Research Center (PEER), the key point is to quantify the conditional probability that a structure would reach or exceed a specified limit state for a given ground motion intensity level. It is worth pointing out that seismic vulnerability analysis of the structure is one of the main research contents of the theoretical performance based earthquake engineering framework.

Seismic vulnerability analysis is a probabilistic evaluation method for the seismic performance of structures(Lagaros, 2008), which quantifies the seismic performance of a structure in a sense of probability and describes the correlation between ground motion (GM) intensity levels and structural damages from a macroscopic view. Intensity measure (IM, as a variable in the analysis) is often used abbreviate to represent the GM intensity levels. The uncertainties of structural response are closely related to IM which were chosen. The selection of IM is particularly important for the seismic vulnerability analysis. At present, the seismic vulnerability researches on bridge structures are mostly based on one IM (Choi *et al*., 2004, Hwang *et al*.,

Correspondence to: Li Ning, School of Civil Engineering, Tianjin University and Key Laboratory of Coast Civil Structure Safety, Ministry of Education, Tianjin 300072, China
Tel: +86-15022396067
E-mail: neallee@tju.edu.cn
†Professor ; ‡Master Student; §Associate Professor

Supported by: National Program on Key Basic Research Project of China (973) under Grant No. 2011CB013603, National Natural Science Foundation of China under Grant Nos. 51378341, 91315301, and Tianjin Municipal Natural Science Foundation under Grant No. 13JCQNJC07200
Received October 16, 2013; **Accepted** May 10, 2014

2001; Moschonas *et al*., 2009), which is referred as a scalar IM. Since the complexity property of GMs, the damage potential may not be characterized by scalar IM effectively. The studies of Baker (Baker, 2007; Baker and Cornell, 2005 and 2008) show that the vector-valued IM (vIM) which includes more than one intensity measure contains more earthquake information and can reflect the uncertainties of ground motions more accurately. Seyedi *et al.*(2010) have made efforts to develop fragility functions for different damage states of an eight-story RC building by vIM. The results illustrated that an increment from one IM to two leads to a significant reduction in the scattering in the vulnerability analysis and allows the uncertainty related to the effect of the second intensity measure to be included in the risk assessments. Koutsourelakis (2010) presented a Bayesian framework to derive vector-valued fragility functions from the limited data available. A statistical-learning model based on logistic regression is proposed to estimate the relative importance of each IM.

Bridge system is composed with different components. The seismic performance of bridge is related to the seismic performance of each component significantly. Here, the component is defined as a member or a set of members of bridge that provide predefined features, which will critically take effect on the seismic performance of bridges. In this paper, the predefined components for bridge model is declared in Section 4. As a system, the bridge structure is more susceptible to damage than any component. The system-level vulnerability of bridges cannot be represented by the vulnerability of single component. To extend reliability bounds, Monte Carlo simulation has been widely used to account for system-level failure events explicitly in the seismic vulnerability analysis of bridges (Kwon and Elnashai, 2010; Nielson, 2005). However, the Monte Carlo simulation may become computationally demanding, because each definition of system-level failure event requires a series numerical simulations. Song and Kang (2009) proposed a matrix-based system reliability method to evaluate different bridge component failure events efficiently while considering bridge component correlations in their response to seismic demands. However, as the number of bridge components N increases, the total number of system events from no component damaged (*no damage state*) to continuous collapse failure of all components (*complete damage state*) increases to 2^N different combinations. There are exponential computational cost required.

The main purpose of this article is to introduce a seismic vulnerability analysis method for bridge structures based on vIM. As an example, a single-bent overpass bridge is taken as the analysis model. Considering the uncertainties related to the bridge itself, ten bridge samples are established statistically with Latin Hypercube sampling approach. Two hundred earthquake GMs are chosen according to the site condition to account for the uncertainties of ground motions (each bridge model randomly combined with 20 GMs). Then, a series of nonlinear dynamic time history analysis are conducted. The uncertainties of capacity and demand are evaluated using the ratios of demands to capacities in different damage states and vector-valued fragility functions of different bridge components are developed. Finally, the system-level vulnerability of the bridge based on vIM is studied with a special correlation matrix model which includes the correlation effects of different bridge components.

2 Seismic vulnerability analysis method for bridge structure based on vIM

2.1 Vector-valued fragility function of bridge component

Vulnerability of a bridge component is defined as the conditional probability that a bridge component reaches or exceeds a predefined damage state for a given ground motion intensity level. It usually can be expressed as

$$P_{\mathrm{f}} = P\left[\frac{S_{\mathrm{d}}}{S_{\mathrm{c}}^{j}} \geq 1\right] = P\left[F_i^j \geq 0\right] \tag{1}$$

where S_{d} is seismic demand, S_{c}^{j} is structural capacity; the safety factor $F_i^j = \ln\left(S_{\mathrm{d}}/S_{\mathrm{c}}^{j}\right)$, P_{f} is failure probability for a specified damage state j of the ith component. Since the random characteristics of both S_{d} and S_{c}^{j} are usually described by a lognormal distribution (Hwang *et al*., 2001; Shinozuka *et al*., 2000) , the safety factor F_i^j follows a normal distribution. If a linear regression analysis between ln (IM) and F_i^j is carried out, the vulnerability for a specified damage state j can be determined by (Pan *et al*., 2007)

$$P_{\mathrm{f}} = P\left[F_i^j \geq 0\right] = \Phi\left(\frac{\mu_{F_i}^j}{\sigma_{F_i}^j}\right) \tag{2}$$

where $\mu_{F_i}^j$ and $\sigma_{F_i}^j$ are mean and standard deviation of the safety factor, F_i^j obtained from the linear regression analysis, $\Phi(\cdot)$ is standard normal cumulative density function. When vIM, which includes two intensity measures IM_1 and IM_2, is used in the seismic vulnerability analysis, $\mu_{F_i}^j$ and $\sigma_{F_i}^j$ can be represented by

$$\mu_{F_i}^j = a\ln\left(\mathrm{IM}_1\right) + b\ln\left(\mathrm{IM}_2\right) + c \tag{3}$$

$$\sigma_{F_i}^j = \sqrt{S_{\mathrm{r}}/(n-3)} \tag{4}$$

where a, b and c are linear regression coefficients, S_{r} is sum of squares of the residuals with respect to the regression plane for scattered points, IM_1 and IM_2 are the first and

second parameters in vIM. Hence, the vector-valued fragility function of a bridge component is finally defined by

$$P_{\mathrm{f}} = \Phi\left(\frac{a\ln(\mathrm{IM}_1)+b\ln(\mathrm{IM}_2)+c}{\sqrt{S_{\mathrm{r}}/(n-3)}}\right) \tag{5}$$

2.2 Vector-valued fragility function of bridge system

Since a bridge is a system composed with various bridge components. Its seismic performance is closely related to the seismic performance of each component. The damages of piers, bearings and abutments will lead to the bridge damage with different potential. Therefore, system-level failure events should be considered when conducting the seismic vulnerability analysis of bridge structures. Studies (Dueñas-Osorio and Padgett, 2011; Song and Kang, 2009) have shown that the bridge structure can be regarded as a series system consisting of different bridge components. It means that if any one of its components damages, the bridge structure will damage. Mathematically, the vulnerability of a bridge system with N components for the jth damage state is expressed as

$$P_{\mathrm{s}}\left(\mathrm{DS}_j \mid \mathrm{vIM}\right) = P\left[\bigcup_{i=1}^{N} E_i\left(\mathrm{DS}_j \mid \mathrm{vIM}\right)\right] \tag{6}$$

where N is number of bridge components; j = {1, 2, 3, 4} and the numbers correspond to *slight*, *moderate*, *extensive* and *complete damage* states; vIM is vector-valued IM; $E_i(\mathrm{DS}_j|\mathrm{vIM})$ is the failure event that the ith bridge component reaches or exceeds the jth damage state for the given vIM.

Generally, a bridge system is composed of N components (each bridge component is tagged by i (i = 1 to N)). A vector with N entries is defined, $\boldsymbol{k} = [k_1, k_2, k_3,\ldots k_{N-1}, k_N]$. Each entry takes values 1 or 0 if the ith bridge component fails or survives, respectively. The totality of such $\boldsymbol{k}$ failure event vectors is contained in the set $\boldsymbol{K}$, whose cardinality is 2^N and includes all possible combinations of bridge component failures. Then, the failure event that a bridge system reaches or exceeds the jth damage state is determined by

$$\boldsymbol{K}_0^j = \left\{\boldsymbol{k} \in \boldsymbol{K},\ \boldsymbol{k} \neq \begin{bmatrix}0 & 0 & 0 & \cdots & 0\end{bmatrix}\right\} \tag{7}$$

Thus, the event that the bridge system survives is

$$\overline{\boldsymbol{K}_o^j} = \left\{\boldsymbol{k} \in \boldsymbol{K},\ \boldsymbol{k} = \begin{bmatrix}0 & 0 & 0 & \cdots & 0\end{bmatrix}\right\} \tag{8}$$

The correlation effect between different bridges components, which will be addressed latter, are ignored here. The vulnerability of the bridge system can be expressed as

$$\begin{aligned} P_{\mathrm{s}}\left(\mathrm{DS}_j \mid \mathrm{vIM}\right) &= 1 - \sum_{\boldsymbol{k}\in\overline{\boldsymbol{K}_o^j}} \prod_{i=1}^{N} P_i\left(\mathrm{DS}_j \mid \mathrm{vIM}\right)^{k_i} \times \left[1 - P_i\left(\mathrm{DS}_j \mid \mathrm{vIM}\right)\right]^{1-k_i} \\ &= 1 - \prod_{i=1}^{N}\left[1 - P_i\left(\mathrm{DS}_j \mid \mathrm{vIM}\right)\right] \\ &= 1 - \prod_{i=1}^{N}\left[\Phi\left(-\frac{a\ln(\mathrm{IM}_1)+b\ln(\mathrm{IM}_2)+c}{\sqrt{S_{\mathrm{r}}/(n-3)}}\right)\right] \end{aligned} \tag{9}$$

$P_i(\mathrm{DS}_j|\mathrm{vIM})$ is the ith bridge component failure probability. Commonly, there is correlation between different bridge components. It will impose errors to vulnerability analysis results if the correlation effect were ignored. To explicitly account for this effect, a special correlation matrix model such as Dunnett-Sobel (DS) class (Dunnett and Sobel, 1955) is proposed. The standardized safety factor $Z_i^j = \left(F_i^j - \mu_{F_i}^j\right)/\sigma_{F_i}^j$ (i = 1 to N) is the DS class standard normal random variable. It means that the correlation coefficient between Z_i^j and Z_k^j is specified as $\rho_{i,k}^j = t_i^j \cdot t_k^j$ for $i \neq k$ and $\rho_{i,k}^j = 1$ for $i = k$. Then, Z_i^j can be represented as

$$Z_i^j = \sqrt{1-(t_i^j)^2}\,U_i + t_i^j X \tag{10}$$

where U_i and X are independent standard normal random variables in the DS class, Z_i^j are conditionally independent of each other for a given outcome $X = x$; t_i^j allows the DS class of standard normal random variables to approximately express the correlation coefficient between bridge components′ standardized safety factors Z_i^j and Z_k^j as $\rho_{i,k}^j = t_i^j \cdot t_k^j$. We can attempt to fit it with a DS class by seeking a set of t_i^j which minimizes the errors between the actual correlations $\rho_{i,k}^j$ and $t_i^j \cdot t_k^j$. According to the random variable Z_i^j, vulnerability of the ith bridge component for given vIM and X is

$$P_i\left(\mathrm{DS}_j \mid X = x, \mathrm{vIM}\right) = 1 - P\left\{F_i^j \le 0\right\} = \Phi\left\{\frac{\dfrac{a\ln(\mathrm{IM}_1)+b\ln(\mathrm{IM}_2)+c}{\sqrt{S_{\mathrm{r}}/(n-3)}} + t_i^j x}{\sqrt{1-(t_i^j)^2}}\right\} \tag{11}$$

Noting that

$$P\left\{F_i^j \le 0\right\} = P\left\{Z_i^j \le -\mu_{F_i}^j/\sigma_{F_i}^j\right\} = P\left\{U_i \le -\frac{\mu_{F_i}^j/\sigma_{F_i}^j + t_i^j x}{\sqrt{1-(t_i^j)^2}}\right\}$$

With the determination of t_i^j, each of the $\boldsymbol{k} \in \boldsymbol{K}_o^j$ event vectors can be estimated for all possible values of X, so the vector-valued fragility function of the bridge system, which accounts for the correlation effects between

different bridge components, is expressed as follows ($\varphi(x)$ = standard normal probability density function)

$$P_s\left(\mathrm{DS}_j \mid \mathrm{vIM}\right)=1-\sum_{\mathbf{k}\in\mathbf{K}_j}\int_{-\infty}^{\infty}\left\{\prod_{i=1}^{N}P_i\left(\mathrm{DS}_j \mid X=x,\mathrm{vIM}\right)^{k_i}\times \left[1-P_i\left(\mathrm{DS}_j \mid X=x,\mathrm{vIM}\right)\right]^{1-k_i}\right\}\varphi(x)\mathrm{d}x$$
$$=1-\int_{-\infty}^{\infty}\left\{\varphi(x)\prod_{i=1}^{N}\left[\Phi\left(-\frac{\frac{a\ln\left(\mathrm{IM}_1\right)+b\ln\left(\mathrm{IM}_2\right)+c}{\sqrt{S_t/(n-3)}}+t_i^j x}{\sqrt{1-\left(t_i^j\right)^2}}\right)\right]\right\}\mathrm{d}x \tag{12}$$

The seismic vulnerability analysis procedure of the bridge structure based on vIM is shown in Fig. 1.

3 Bridge model and modeling consideration

3.1 The two span single-bent overpass bridge model

A two span single-bent overpass bridge is taken as the research object and the length of span is 44 m for each span. C50 concrete is used in the superstructure which is supported on a reinforced concrete two-column bent. The width and height of the box girder is 16.4 m and 1.75 m, the cross area is 8.268 m^2, the bending moment of inertia of girder section about vertical axis and horizontal axis is 122.9 m^4 and 2.901 m^4, and the torsional moment of inertia of girder section is 11.8 m^4, respectively. Polytetrafluoroethylene (PTEF) sliding bearings are seated on the abutments with U-shaped wing walls. The piers are solid circular columns with a height of 12 m and a diameter of 1.65 m and their concrete strength grades are C40. Longitudinal and spiral reinforcements are specified as HRB335 and their reinforcement ratios are 1.2% and 0.8%. The site condition is II in Chinese seismic code.

In this study, the three-dimensional finite-element model of the bridge is created in OpenSees platform (OpenSees, 2012). The decks and the box-girders are combined together and simulated with elastic beam-column element. Beams with hinges elements are used to model the piers. The interaction of pile-soil-structure is taken into account (Penzien *et al*., 1964). *P-Δ* effects are included. Generally, the selection of an appropriate abutment model has great influences on nonlinear behavior of the bridge structure under earthquakes, especially on the short and medium span bridges (Aviram *et al*., 2008). To reflect the dynamic response characteristics of abutments, spring abutment model proposed by Mackie (Aviram *et al*., 2008) is used. To be clarify, the spatial seismic excitation effect is not taken into account. For more complicated bridge model, the reader could referred to Sextos′ work (Sextos *et al*., 2003). The nonlinear analysis model of the bridge is shown in Fig. 2. It must be noted that the two span single-bent overpass bridge′s pier in the sketch (Fig. 2.) is plotted twice, one for geometry illustration and one for simplified model.

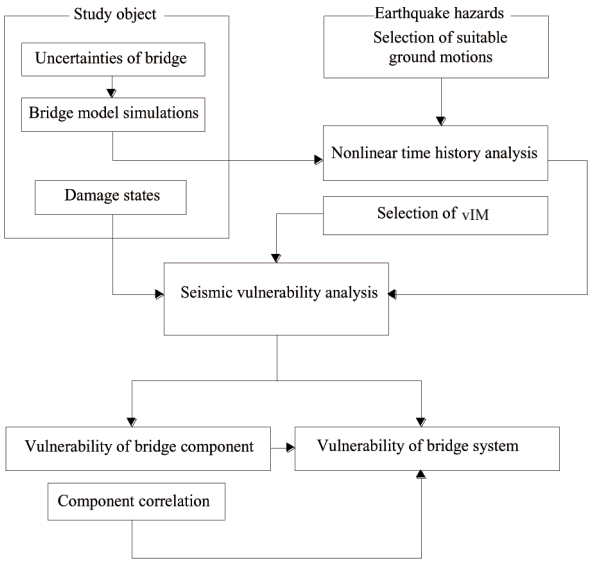

Fig. 1 Seismic vulnerability analysis procedure of the bridge structure based on vIM

3.2 Consideration of the uncertainties of bridge itself

Uncertainties of a bridge are mainly related to the parameters of materials, such as the variability of steel and concrete, and often leads to the uncertainties of structural dynamic characteristics including natural periods and vibration modes. Furthermore, it will result in the uncertainties of structural dynamic responses. The existing research (Kwon and Elnashai, 2006) has shown that uncertainties of the structure have great influence on its dynamic response. A parametritc analysis carried out by Pan *et al*. (2007) illustrated that bridge response is sensitive to uncertainties associated with material parameters such as superstructure weight, concrete compressive strength and reinforcement yield strength. According to statistical properties of construction materials, Latin Hypercube sampling approach (Wyss and Jorgensen, 1998) is used to account for the uncertainties of the three parameters mentioned above in

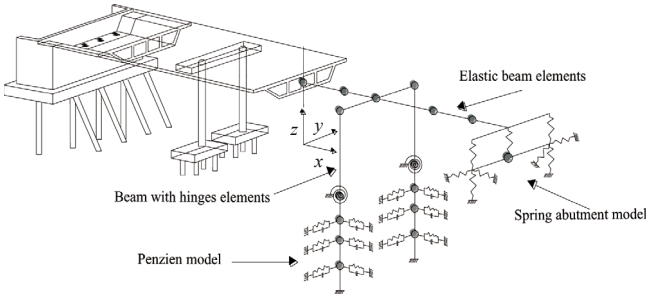

Fig. 2 Nonlinear analysis model of the single-bent overpass

this approach. Each parameter is described by a normal distribution variable and the probability density function of each random variable is divided into a histogram with equal probability intervals graded linearly corresponding to cumulative distributions varying from 5% to 95%. The statistical information of variables is shown in Table 1. Then, 10 nonlinear analysis models of the bridge were built.

3.3 Selection of ground motions

A key factor of seismic vulnerability analysis is the input ground motions, which is the basis of structural seismic analysis. There are significant differences in structural response when a bridge suffers different earthquakes. To perform the vulnerability analysis, various hazard levels of ground motions need to be adopted to evaluate the probability that a bridge experiencing certain damage state within a given return period. These earthquake records should be representative of the seismic characteristics of the specified site condition. Because there are differences between Chinese and American seismic codes, earthquake records selected from the strong motion database of PEER cannot be used directly. To obtain earthquake records satisfied the site condition Class II in Chinese seismic code (thickness of sediment layer $h_d \geq 5$ m with equivalent shear wave speed v_s satisfy 250 m/s $< v_s <$ 500 m/s; or 3 m $< h_d <$ 50 m with 150 m/s $< v_s <$ 250 m/s, or 3 m $< h_d <$ 15 m with $v_s \leq$ 150 m/s), the method proposed by Lv and Zhao (2007) is adopted, which provide the relationship of site conditions between China and U.S. by comparison of the soil classified parameters, and proposed a modification procedure for US site condition when it is adopted in China. Then, 200 earthquake records (for different hazard levels) are chosen for seismic vulnerability analysis. General properties of these records are, (1) fault distance range: 20–200 km; (2) moment magnitude range: 6.5–7.6; (3) shear wave velocity range: 260–510 m/s; (4) no velocity pulse effect. General properties and PGA distribution of 200 earthquake records are shown in Table 2 and Fig. 3.

To reflect the randomness of earthquakes, 200 earthquake records are divided into ten groups with twenty records each. Therefore, it is possible to randomly assign these groups of earthquake records to the ten established bridge models. Finally, we can get 200 groups of bridge-earthquake samples. The nonlinear time history analysis for 200 samples in x (longitude) direction, as well as in y (transverse) direction of bridge, is conducted on the Open System for Earthquake Engineering Simulation platform (OpenSees, 2012).

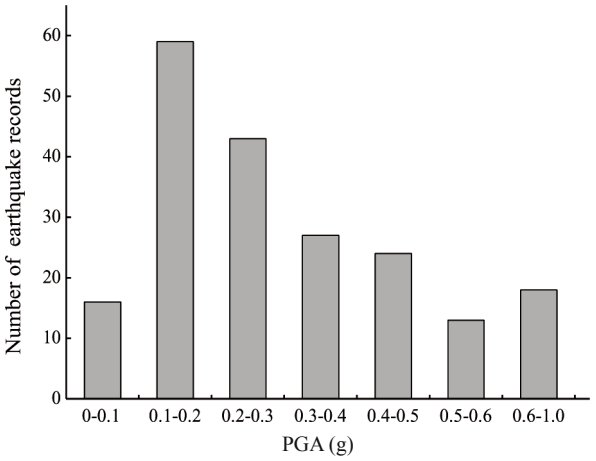

Fig. 3 PGA distribution of two hundred earthquake records

Table 1 Statistical information of variables

Variables	Distribution	Mean	Variation coefficient
w (kN/m^3)	Normal distribution	26.25	0.1
f_y (MPa)	Normal distribution	263.48	0.072
f_c (MPa)	Normal distribution	33.30	0.12

Table 2 General properties of two hundred earthquake records

Earthquake name	Fault distance range (km)	Moment magnitude	Shear wave velocity range (km/s)	Velocity pulse	Number of earthquake records
San Fernando (1971)	22–193	6.6	271–453	None	25
Imperial Valley (1979)	32–85	6.5	275–362	None	12
Loma Prieta (1989)	28–117	6.9	271–478	None	26
Landers (1992)	54–190	7.3	270–446	None	48
Northridge (1994)	31–144	6.7	301–445	None	21
Duzce, Turkey (1999)	34–183	7.1	274–425	None	14
Chi-Chi, Chinese Taipei (1999)	24–120	7.6	262–504	None	54
Total					200

3.4 Damage states definition

The structures or structural components may undergo different damage stage in the design process based on performance states for different performance targets. To assess the seismic vulnerability of a bridge, the damage state must be determined. Furthermore, the damage indexes also need to be quantified. According to HAZUS 99 (HAZUS99, 1999), seismic damage states of a bridge can be classified into five: *no damage*, *slight damage*, *moderate damage*, *extensive damage* and *complete damage* (collapse). Because bridge is a system composed by different components, damages of piers, bearings and abutments all possess damage potential to the bridge system-level damage. In this study, damage indexes of each bridge component, which correspond to the five damage states, are first defined.

Damage states for piers are determined using the relative displacement ductility ratio of a pier, which is defined by (Hwang *et al*., 2001)

$$\mu_{\mathrm{d}} = \frac{\Delta}{\Delta_{\mathrm{cy1}}} \tag{13}$$

where Δ is the relative displacement at the top of a pier obtained from seismic response analysis; Δ_{cy1} is the relative displacement of a pier when the vertical reinforcing steel bars at the bottom of the pier reach the first yield. The five damage states are quantified in terms of the relative displacement ductility ratios as shown in Table 3. In Table 3, μ_{cy1} is the first yield displacement ductility ratio; μ_{cy} is the yield displacement ductility ratio (which corresponding to the rotation curvature at the plastic hinge region equal to φ_{y}, which is the equivalent yield curvature, the readers may be referred to Priestley *et al*. (2007)); μ_{c4} is the displacement ductility ratio with $\varepsilon_{\mathrm{c}} = 0.004$ (concrete compression strain at the bottom of pier edges); μ_{cmax} is the maximum displacement ductility ratio, which can be expressed as $\mu_{\mathrm{cmax}} = \mu_{\mathrm{c4}}+3$ (Buckle *et al*., 2006). It is noted that the displacement ductility ratio is defined in terms of the first yield displacement, so μ_{cy1} is equal to 1.

Based on the research results of Nielson (2005), damage indexes of PTEF sliding bearings and abutments measured by displacements are defined, as shown in Table 4. μ_{cdL} is the displacement of PTEF sliding bearings in longitudinal direction; μ_{cdT} is the displacement of PTEF sliding bearings in transverse direction; μ_{cabP} is the displacement of abutments in passive action; μ_{cabA} is the displacement of abutments in active action; μ_{cabT} is the displacement of abutments in transverse direction.

4 vIM based seismic vulnerability analysis of the single-bent overpass bridge

The single-bent overpass has seven components which correspond to columns in longitudinal direction, columns in transverse direction, PTEF sliding bearings in longitudinal direction, PTEF sliding bearings in transverse direction, abutments in passive action, abutments in active action and abutments in transverse direction. Each component of the bridge is indexed by i (i = 1 to 7).

4.1 Selection of vIM

In this study, vIM with two intensity measures, IM_1 and IM_2, was adopted to perform the seismic vulnerability analysis of the bridge. The selection principle of the two parameters is to make sure that both of them are strongly correlated with the safety factor F_i^j. On the other hand, the correlation between the two measures should be as small as possible.

The nonlinear time history analysis of the 10 sample bridges has been carried out using 200 earthquake records. Each bridge was analyzed for twenty different records selected to cover a wide range of PGAs. So a total of two hundred analysis cases have been performed. According to the analysis results and the basic characteristics of the two hundred earthquake records, the correlation coefficients between ln (IM)s and the safety factors F_i^2 in *moderate damage* state, as well as the correlation coefficients between different IMs, are calculated, as shown in Table 5 and Table 6.

It can be seen from Table 5–6, the above two conditions often cannot be satisfied simultaneously. Considering these two conditions synthetically, $S_a(T_1)$ (The spectral acceleration at the first period) and $S_a(T_2)$ (The spectral acceleration at the second period) are chosen as the two parameters of vector-valued IM, that is vIM = ($S_a(T_1)$, $S_a(T_2)$). It should be noted that the

Table 3 Damage states of piers measured by the relative displacement ductility ratios

Damage states	Criteria
No damage	$\mu_{\mathrm{d}} < \mu_{\mathrm{cy1}}$
Slight damage	$\mu_{\mathrm{cy1}} \le \mu_{\mathrm{d}} < \mu_{\mathrm{cy}}$
Moderate damage	$\mu_{\mathrm{cy}} \le \mu_{\mathrm{d}} < \mu_{\mathrm{c4}}$
Extensive damage	$\mu_{\mathrm{c4}} \le \mu_{\mathrm{d}} < \mu_{\mathrm{cmax}}$
Complete damage	$\mu_{\mathrm{d}} \ge \mu_{\mathrm{cmax}}$

Table 4 Damage states of PTEF sliding bearings and abutments measured by displacements

Damage indexs	Slight damage	Moderate damage	Extensive damage	Complete damage
μ_{cdL}(mm)	100	150	200	500
μ_{cdT}(mm)	100	150	200	500
μ_{cabP}(mm)	37	146	-	-
μ_{cabA}(mm)	9.8	37.9	77.2	-
μ_{cabT}(mm)	9.8	37.9	77.2	-

Table 5 Correlation coefficients between ln (IM)s′ and the safety factors F_i^2 in moderate damage state

	F_1^2	F_2^2	F_3^2	F_4^2	F_5^2	F_6^2	F_7^2
ln(PGA)	0.758	0.690	0.780	0.642	0.853	0.883	0.902
ln(PGV)	0.847	0.847	0.849	0.836	0.690	0.597	0.635
ln(PGD)	0.431	0.426	0.415	0.437	0.289	0.188	0.183
ln($S_a(T_1)$)	0.955	0.883	0.944	0.841	0.634	0.543	0.578
ln($S_a(T_2)$)	0.818	0.743	0.825	0.714	0.645	0.620	0.629
ln(PGV/PGA)	0.262	0.296	0.260	0.284	0.305	0.237	0.217

Table 6 Correlation coefficients between different IMs

	PGA	PGV	PGD	$S_a(T_1)$	$S_a(T_2)$	PGV/PGA
PGA	1	0.700	0.214	0.717	0.780	0.274
PGV	0.700	1	0.597	0.820	0.738	0.304
PGD	0.214	0.597	1	0.380	0.360	0.186
$S_a(T_1)$	0.717	0.820	0.380	1	0.798	0.260
$S_a(T_2)$	0.780	0.738	0.360	0.798	1	0.288
PGV/PGA	0.274	0.304	0.186	0.260	0.288	1

power-law form multi-spectral values IM and spectral shape IM (Vamvatsikos and Cornell, 2005) also take into account more than one spectral information. However, vIM does not only decrease dispersion but also lead to the fragility surface which provide a direct visualization of the spectral shape′s influence on the capacities for fragility analysis of structures. In this paper, the first two vibration modes of the bridge are, $T_1 = 0.98$ s (longitude vibration along the bridge), $T_2 = 0.74$ s (transverse vibration).

4.2 Vulnerability of bridge component

Based on the results of the nonlinear time history analysis, a regression analysis is performed to establish a relationship between the safety factors F_i^2 in *moderate damage* state, $\ln\left(S_a\left(T_1\right)\right)$, and $\ln\left(S_a\left(T_2\right)\right)$. Then, vector-valued fragility functions of different bridge components can be obtained by Eq. (5). Regression models and vector-valued fragility functions of different bridge components is shown in Table 7.

Although vIM = ($S_a(T_1)$, $S_a(T_2)$) seems to be more effective for the estimation of structural damages and it is also well adapted to vector-valued probabilistic seismic hazard assessment proposed by Bazzurro and Cornell (2002), $S_a(T_1)$ and $S_a(T_2)$ are strongly correlated ($R = 0.798$). Due to the strong correlation between the two parameters, data points usually do not cover the whole space defined by $S_a(T_1)$-$S_a(T_2)$. So it will lead to serious errors if we consider the whole space as the domain of independent variables for vector-valued fragility functions. To account for the correlation effects of the two IMs, a method suggested by Gehl *et al.* (2013) is used. In this method, a regression analysis with 95% confidence levels is performed between $S_a(T_1)$ and $S_a(T_2)$ using the data points corresponding to the two hundred earthquake records, as shown in Fig. 4. The median line represents the linear relation between the two parameters. Two dotted lines are the lower and upper bounds of 95% confidence intervals. Then, the area between the confidence intervals can be considered as the validity domain of independent variables for vector-valued fragility functions.

4.3 Comparison between scalar IM and vIM

Fragility curves are generally developed using one intensity measure, referred as scalar IM, to relate the level of shaking intensity to the expected structural damages. When the ground motions are represented by vIM, which includes two intensity measures (such as $S_a(T_1)$ and $S_a(T_2)$), fragility curves will become fragility surfaces. The goal of this section is to illustrate that vIM is more effective for estimating bridge damages than scalar IM. Table 8 shows standard deviations of the fragility functions based on scalar IM and vIM for different bridge components in *moderate damage* state. We can see that the standard deviations of vector-valued fragility functions are smaller than single-variable fragility functions. It indicates that an increment of IM from one to two IMs results in a significant reduction in the dispersion in the vulnerability analysis of the bridge structure.

To appropriately illustrate the difference between single-variable fragility curves and vector-valued fragility surfaces, a fragility surface need to be transformed into fragility curves which usually can be

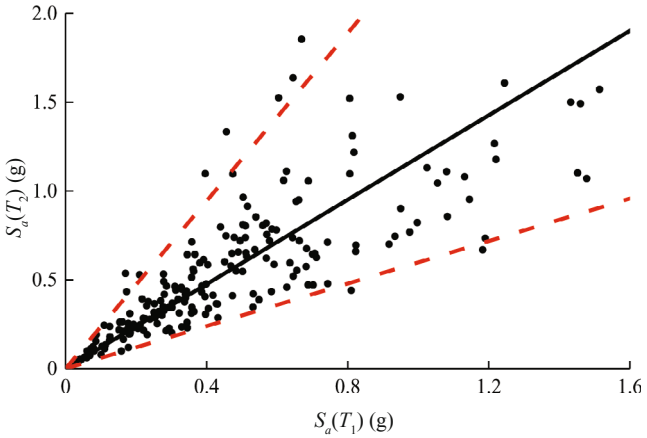

Fig. 4 Correlation analysis between $S_a(T_1)$ and $S_a(T_2)$

Table 7 Regression models and vector-valued fragility functions of different bridge components in moderate damage state

Component number	Regression models	Standard deviation $\sigma^2_{F_i}$	Vector-valued fragility functions
1	$\mu^2_{F_1}=\ln(F_1^2)=0.763\times\ln(S_a(T_1))+0.11\times\ln(S_a(T_2))+0.446$	0.13665	$P_1=\Phi(\mu^2_{F_1}/\sigma^2_{F_1})$
2	$\mu^2_{F_2}=\ln(F_2^2)=0.727\times\ln(S_a(T_1))+0.311\times\ln(S_a(T_2))+0.775$	0.25991	$P_2=\Phi(\mu^2_{F_2}/\sigma^2_{F_2})$
3	$\mu^2_{F_3}=\ln(F_3^2)=0.650\times\ln(S_a(T_1))+0.148\times\ln(S_a(T_2))+0.484$	0.13566	$P_3=\Phi(\mu^2_{F_3}/\sigma^2_{F_3})$
4	$\mu^2_{F_4}=\ln(F_4^2)=0.676\times\ln(S_a(T_1))+0.277\times\ln(S_a(T_2))+0.16$	0.32047	$P_4=\Phi(\mu^2_{F_4}/\sigma^2_{F_4})$
5	$\mu^2_{F_5}=\ln(F_5^2)=0.355\times\ln(S_a(T_1))+0.367\times\ln(S_a(T_2))-0.961$	0.40461	$P_5=\Phi(\mu^2_{F_5}/\sigma^2_{F_5})$
6	$\mu^2_{F_6}=\ln(F_6^2)=0.114\times\ln(S_a(T_1))+0.546\times\ln(S_a(T_2))-0.648$	0.45179	$P_6=\Phi(\mu^2_{F_6}/\sigma^2_{F_6})$
7	$\mu^2_{F_7}=\ln(F_7^2)=0.069\times\ln(S_a(T_1))+0.594\times\ln(S_a(T_2))-0.686$	0.43303	$P_7=\Phi(\mu^2_{F_7}/\sigma^2_{F_7})$

Table 8 Standard deviations of fragility functions based on scalar IM and vIM for different bridge components in moderate damage state

Component number	Standard deviations		
	scalar IM		vIM
	$S_a(T_1)$	$S_a(T_2)$	$(S_a(T_1), S_a(T_2))$
1	0.20118	0.29339	0.13665
2	0.31929	0.35854	0.25991
3	0.20408	0.25941	0.13566
4	0.35277	0.39398	0.32047
5	0.49179	0.48134	0.40461
6	0.55607	0.53230	0.45179
7	0.52524	0.50258	0.43303

plotted with respect to one intensity measure by fixing the second one. However, $S_a(T_1)$ and $S_a(T_2)$ are strongly correlated. Developing the single-variable fragility curves with one intensity measure while keeping the other one constant, it will lead to erroneous conclusions, especially for extreme limit-state. So the method proposed by Gehl *et al*. (2013), which is to cut slices along the affine lines within the validity domain of independent variables for vector-valued fragility functions, is used to obtain the transformed fragility curves. Then, the first bridge component (Columns in longitudinal direction, component 1 defined in this section previously) is taken as the example.

The comparison of the single-variable fragility curve and slices of the vector-valued fragility surface in moderate damage state is shown in Fig. 5.

The result shows that single-variable fragility curve cannot represent the effects of a second intensity measure on the seismic behavior of the bridge. If there is only one intensity measure used in the seismic vulnerability analysis, an average curve will be developed and it will not incorporate the variability due to the other characteristics of ground motions. Vector-valued fragility surface can propagate the effects of a second intensity measure in the result. Also, it allows the uncertainties related to the effects of the second intensity measure to be considered within risk assessment. Its superiority is obviously that fragility surface can reflect the damage levels of the bridge structure better.

4.4 Vulnerability of bridge system

The correlation coefficient between the standardized safety factors Z_i^j and Z_k^j for a specified damage state j is expressed as

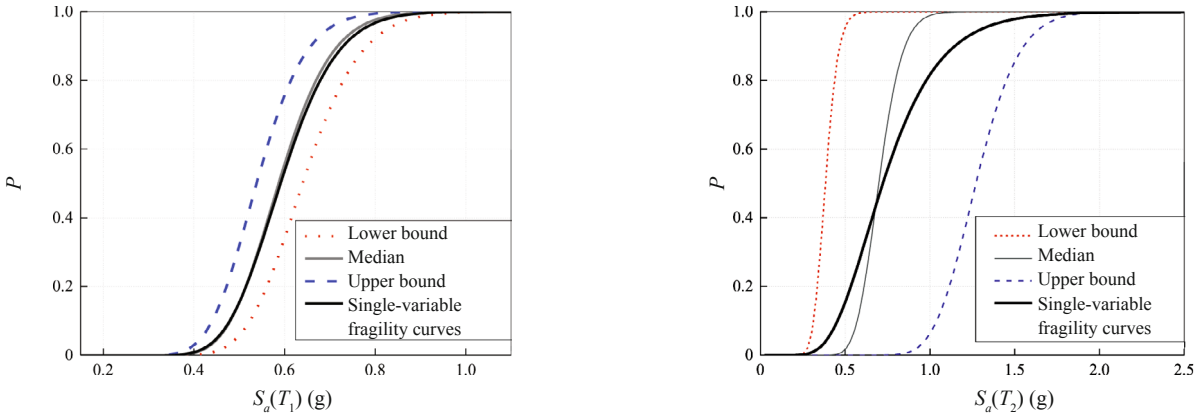

Fig. 5 Comparison of the single-valued fragility curve and slices of the vector-valued fragility surface (median line representing the linear relation between $S_a(T_1)$ and $S_a(T_2)$, the lower and upper bounds of 95% confidence intervals) in moderate damage state

$$\rho^{j}_{Z_i,Z_k}=\rho^{j}_{F_i,F_k}=\frac{\mathrm{COV}\left(F_i^j,F_k^j\right)}{\sigma^{j}_{F_i}\cdot\sigma^{j}_{F_k}}=\frac{E\left[\left(F_i^j-\mu^{j}_{F_i}\right)\left(F_k^j-\mu^{j}_{F_k}\right)\right]}{\sigma^{j}_{F_i}\cdot\sigma^{j}_{F_k}} \tag{14}$$

The correlation coefficients $\rho^2_{Z_i,Z_k}$ between different bridge components in *moderate damage* state can be obtained by Eq. (14). Table 9 shows the computed correlation coefficients $\rho^2_{Z_i,Z_k}$. To achieve the suitable values of t_i^2, a DS class correlation matrix which fits the correlation coefficients $\rho^2_{Z_i,Z_k}$ with the least sum-of-squared-errors is found. The approximated correlation matrix is provided in Table 10 for comparison.

As can be seen from Table 9–10, the computed correlation matrix is approximated by a DS class matrix with small errors. In this condition, the values of t_i^2 for *moderate damage* state are 0.9775, 0.9150, 0.6005, 0.8936, 0.7992, 0.4999, 0.5321. Based on the vector-valued fragility functions of different bridge components in Table 7 and the values of t_i^2, the vector-valued fragility function of the bridge system can be obtained by Eq. (12). Then, the fragility surface of the bridge system in *moderate damage* state can be plotted, as shown in Fig. 6.

To verify the validity of the vector-valued fragility function of the bridge system, a Monte Carlo simulation (MCS) approach using the same demand and capacity models is adopted. Then, two single-variable fragility curves can be obtained by cutting slices along the lower and upper boundary of the fragility surface. Figure 7 shows two single-variable fragility curves obtained by slices of the fragility surface of the bridge system and the MCS result, and they fits very well. The result further illustrated the validity of the vector-valued fragility function for bridge system.

By comparing the vulnerability of different bridge component, it is found that component 3 (PTEF sliding bearings in longitudinal direction) is more vulnerable to earthquake damage than any other bridge component. So we can illustrate the difference between the system vulnerability and the component vulnerability by just considering component 3 only. Figure 8 shows contour distributions of the vulnerability of the bridge system and component 3.

It can be seen from Fig. 8 that for any given value of vIM($S_a(T_1)$, $S_a(T_2)$), the vulnerability failure probability of the bridge system is significantly greater than component 3. The result indicates that a bridge system

Table 9 Correlation coefficient matrix for standardized safety factors of different bridge Components in moderate damage state

	Z_1^2	Z_2^2	Z_3^2	Z_4^2	Z_5^2	Z_6^2	Z_7^2
Z_1^2	1	0.881	0.601	0.861	0.808	0.486	0.511
Z_2^2	0.881	1	0.526	0.886	0.699	0.440	0.488
Z_3^2	0.601	0.526	1	0.531	0.505	0.296	0.310
Z_4^2	0.861	0.886	0.531	1	0.670	0.424	0.475
Z_5^2	0.808	0.699	0.505	0.670	1	0.444	0.436
Z_6^2	0.486	0.440	0.296	0.424	0.444	1	0.277
Z_7^2	0.511	0.488	0.310	0.475	0.436	0.277	1

Table 10 Correlation coefficient matrix for standardized safety factors of different bridge components in moderate damage state approximated by DS class

	Z_1^2	Z_2^2	Z_3^2	Z_4^2	Z_5^2	Z_6^2	Z_7^2
Z_1^2	1	0.894	0.587	0.873	0.781	0.487	0.520
Z_2^2	0.894	1	0.549	0.818	0.731	0.457	0.487
Z_3^2	0.587	0.549	1	0.537	0.480	0.300	0.320
Z_4^2	0.873	0.818	0.537	1	0.714	0.447	0.475
Z_5^2	0.781	0.731	0.480	0.714	1	0.400	0.425
Z_6^2	0.487	0.457	0.300	0.447	0.400	1	0.266
Z_7^2	0.520	0.487	0.320	0.475	0.425	0.266	1

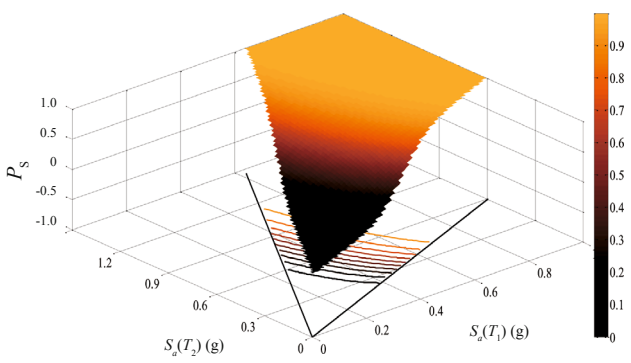

Fig. 6 Fragility surface of the bridge system in moderate damage state

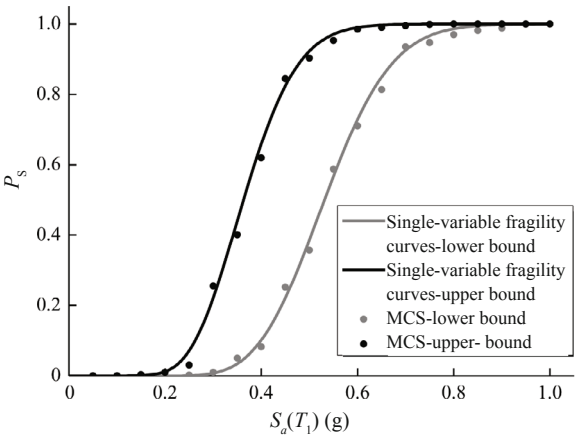

Fig. 7 Two single-variable fragility curves obtained by slices of the fragility surface (the lower and upper bounds of 95% confidence intervals) of the bridge system and the Monte Carlo simulation (MCS) routines

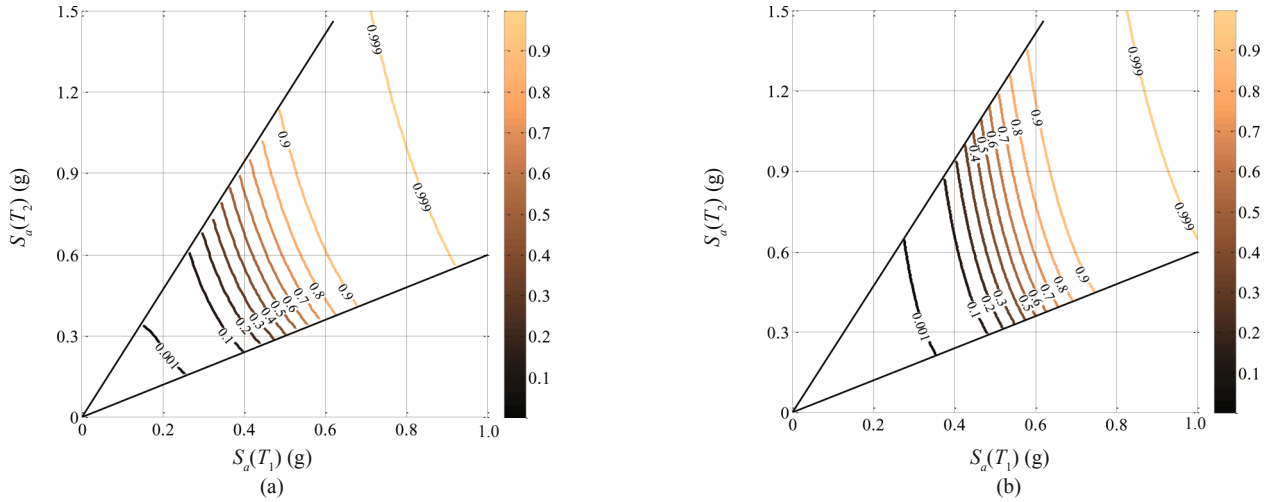

Fig. 8 Comparative analysis of (a) the vulnerability of the bridge system and (b) the vulnerability of Component 3

is more vulnerable to earthquake damage than any other components. If the seismic vulnerability of the bridge structure is represented by the vulnerability of single component, it will overestimate the seismic performance of the bridge. The component vulnerability cannot reflect the real seismic performance of the bridge structure and the system level failure events must be taken into account when performing the seismic vulnerability analysis for the bridge structures.

5 Conclusions

Current methods used to perform the seismic vulnerability analysis of the bridge structure often represent the ground motions intensity by one intensity measure, which cannot accurately characterize the seismic damage potential to bridge structure relevant to seismic intensity measure.

A fragility analysis method for the vulnerability of the bridge system based on vIM with a special correlation matrix model which includes the correlation effects of different bridge components is presented. The research results show that an increment of IM from one (scalar IM) to two (vIM) leads to a significant reduction in the scatter of the fragility functions and a potential reduction in the uncertainties for evaluating earthquake risk consequently. The vector-valued fragility functions developed by vIM can propagate the effects of a second intensity measure and allows the uncertainties related to the effects of the second intensity measure to be considered within risk assessments, they can reflect the damage levels of the bridge structure better.

Bridge structure consists of different components, and its seismic performance is closely related to the seismic performance of each component. By studying the vulnerability of the bridge system, it indicates that Dunnett–Sobel class correlation matrix model can account for the correlation effects of different bridge components better. As a system, the bridge is more vulnerable to earthquake damages than any other components, the system-level failure events must be taken into account when performing the seismic vulnerability analysis of the bridges.

References

Aviram A, Mackie K and Stojadinovic B (2008), "Effect of Abutment Modeling on the Seismic Response of Bridge Structures," *Earthquake Engineering and Engineering Vibration*, **7**(4): 395–402.

Baker JW (2007), "Probabilistic Structural Response Assessment Using Vector-valued Intensity Measures," *Earthquake Engineering & Structural Dynamics*, **36**(13): 1861–1883.

Baker JW and Cornell CA (2005), "A Vector-valued Ground Motion Intensity Measure Consisting of Spectral Acceleration and Epsilon," E*arthquake Engineering & Structural Dynamics*, **34**(10): 1193–1217.

Baker JW and Cornell CA (2008), "Vector-valued Intensity Measures Incorporating Spectral Shape for Prediction of Structural Response," *Journal of Earthquake Engineering*, **12**(4): 534–554.

Bazzurro P and Cornell CA (2002), "Vector-valued Probabilistic Seismic Hazard Analysis," *Proceedings of 7th U.S. National Conference on Earthquake Engineering*, Paper No. 61.

Buckle I, Friedland I and Mander J, *et al*. (2006), *Seismic Retrofitting Manual for Highway Structures: Part 1-Bridges*, Multidisciplinary Center for Earthquake Engineering Research, State University of New York.

Choi E, DesRoches R, and Nielson BG (2004), "Seismic Fragility of Typical Bridges in Moderate Seismic Zones," *Engineering Structures*, **26**(2): 187–199.

Dueñas-Osorio L and Padgett J (2011), "Seismic Reliability Assessment of Bridges with User-defined System Failure Events," *Journal of Engineering*